RELATIVE REACTIVITIES IN THE ELECTROCHEMICAL OXIDATION OF HYDROCARBON FUEL COMPONENTS

Eugene Luksha and Eugene Y. Weissman

General Electric Co.
Direct Energy Conversion Operation
West Lynn, Massachusetts 01905

Introduction

The tolerance of a fuel cell anode to n-octane containing various types of hydrocarbon additives, aromatic, olefinic, and naphthenic was determined (1). It was found that the octane-based fuel of the composition shown in Table 1 behaved very similarly (50 mv or less difference), at least on a short term basis, to n-octane alone.

Table 1

Model Hydrocarbon Fuel Cell Fuel

Compound Type	Concentration Mole %
Olefins	0-5
Aromatics	1
Naphthenes (cyclohexane type)	5
(cyclopentane type)	15
n + i octane	balance

If the reactivities of each one of the fuel components in Table 1 are different it can be inferred that anodic oxidation will proceed, at steady-state, according to the extent of electrode coverage by the most reactive species. This implies, of course, that probably a major portion of the anode will be covered by more refractory species; these may be present in the original fuel and may also consist of reaction intermediates.

Experimental

The details of the experimental features were outlined earlier (1). The following additional procedures apply specifically to this case:

A fuel, after making a single pass through the fuel cell (anode compartment value 7.5 cm^3), was passed, with its oxidation products, into a Perkin-Elmer 801 gas chromatograph, equipped with a heated gas sampling valve and a differential flame ionization detector. The chromatographic measurements of the exhaust composition were made after the cell was operated for long enough to eliminate biases introduced by concentration gradients in the exhaust system and/or adsorption effects. The gas chromatograph was calibrated before each measurement by injecting several fuels in the concentration range of interest to determine retention times, peak heights, and areas. The gas chromatograph was operated isothermally at 100°C and the calibrations were made in terms of peak areas determined with a disc integrator fitted on a Leeds and Northrup 5 mv recorder. The column, prepared by Perkin-Elmer was a 12 foot, 1/8 inch o. d. Stainless steel tube packed with 10 wt. % Apiezon-L supported on 80-100 mesh chromosorb W. Helium gas was used as a carrier, air and hydrogen gases were used for the flame detector. All were zero grade (hydrocarbon free) supplied by Matheson.

Since all the fuels used in this study are liquids at room temperature, the sample valve, sampling tube, and the fuel exhaust lines were heated to prevent condensation. The temperatures of the lines were maintained at about 130°C and monitored frequently with the aid of appropriately positioned thermocouples.

Prior to entering the hot lines, the anode exhaust passed through a heated electrolyte trap made of Teflon. Fuel flows in the microliter range were measured with a capillary tube flowmeter. A schematic diagram of this system is shown in Figure 1.

Measurements of the inlet fuel flow, the cell current, and the exhaust composition supplied all the data that were necessary to calculate the current contributions of each component in the binary fuel. However, since a flame ionization detector was employed, it was not possible to measure the CO_2 or H_2O in the exhaust stream. Therefore, the concentrations measured only refer to mixtures of hydrocarbon components. The calculations were performed on a General Electric 625 computer using programs written in Fortran IV. The complete programs are given elsewhere (2).

The anodes were platinum-Teflon-screen composites of a type described in the literature (3). They were of 3 x 3 inch (0.05 ft^2) active geometric area. The electrolyte was phosphoric acid, maintained at 95 wt. % by controlled addition of water. All measurements were made at 350°F.

The anodes were operated, for the most part, at potentials in the range of 0.5 volt vs. H_2/H^+; this is a practical potential at which hydrocarbon anodes can be operated for extended periods with reasonable power outputs (1).

Results

A. Binary Fuels

1. Aromatic Additive (benzene/n-octane)

To study the relative reactivity of aromatics and n-paraffins, a binary fuel consisting of benzene + n-octane was examined.

For this particular fuel the benzene concentration was varied from 1 to 5 mole %, and the liquid fuel flow rate was varied from 5 to 40 μ l/min. For n-octane, this corresponds to at least two times the stoichiometric amount for all cases. The experimental results for all the benzene/n-octane mixtures studied are summarized in Table 2. Columns 4 and 7, respectively, give the exhaust composition of the cell and the current contribution from benzene. A comparison of columns 1 and 4 indicates that benzene is preferentially oxidized. In Figure 2 the quantity I_A/I_T the current fraction from benzene, is plotted against the fuel flow rate for a fuel consisting of 99 mole % n-octane + 1 mole % benzene. These data points were obtained at an essentially constant current (~1.5 amps) and anode potential (~0.5 volt vs. N.H.E.). The current fraction from benzene is directly proportional to the fuel flow rate. This indicates that the aromatic is consumed as rapidly as it is supplied, at least for the range of flow rates studied, and provided that $I_T > I_A$.

Further generalization is provided by Figure 3 which is a plot of I_A, the current from benzene, vs. the benzene flow rate, for fuels consisting of n-octane + 1, 3, and 5 mole % benzene. The current from benzene is proportional to the benzene flow rates, again indicating that the aromatic is consumed as rapidly as it is supplied, independent of whether it is supplied at high concentrations and low total fuel flow rates or low concentrations and high total fuel flow rates.

Table 2

Current Contribution and Exhaust Composition for Benzene

Inlet Fuel Composition, mole %	Liquid Fuel Flow Rate, μl/min.	Benzene Flow Rate, mole/min. x 10^6	Benzene Concentration in Exhaust, mole % x 10^2	Total Current, I_T - amp	Anode Potential vs. H_2/H^+, volt	Current from Benzene, I_A - amp
99% n-octane + 1% benzene	5	0.313	13.0	1.46	0.510	0.014
	11	0.688	5.0	1.55	0.447	0.032
	20	1.25	5.3	1.53	0.525	0.047
	30	1.88	4.6	1.52	0.456	0.087
	38	2.38	4.39	1.52	0.550	0.110
	40	2.48	26.8	0.49	0.505	0.089
	40	2.48	29.2	0.49	-----	0.086
	40	2.48	16.5	1.01	0.530	0.101
	40	2.48	15.6	1.01	0.525	0.102
	40	2.48	10.9	1.46	0.514	0.108
	40	2.48	11.7	1.44	0.540	0.107
	40	2.48	16.9	1.50	0.525	0.101
	40	2.48	14.7	1.51	0.500	0.104
	40	2.48	7.95	2.03	0.490	0.111
	40	2.48	6.55	2.00	0.510	0.113
	40	2.48	5.35	2.00	0.480	0.114
	40	2.48	7.62	2.52	0.520	0.112
	40	2.48	6.35	2.49	0.497	0.113
	40	2.48	5.55	2.97	0.500	0.114
	40	2.48	4.97	3.01	0.500	0.114
97% n-octane + 3% benzene	10	1.87	17.8	0.78	0.485	0.085
	20	3.73	9.72	2.54	0.535	0.176
	30	5.62	26.8	1.26	0.540	0.25
	38	7.03	23.5	1.39	0.535	0.315
95% n-octane + 5% benzene	10	3.15	24.5	0.75	0.502	0.146

The current contribution from benzene, I_A, under these conditions can be represented by the relation:

$$I_A = 4.51 \times 10^4 V_A \quad (1)$$

where V_A is the benzene flow rate in units of gm. mole/min.

If this result can be generalized to all aromatics, at these conditions of operation, the following relationship can be obtained:

$$I_A = 0.934\, nF\, u N_A \quad (2)$$

where:

u = mole feed rate, moles per minute
N_A = mole fraction of aromatic in feed stream

and the other terms have their usual significance.

2. Olefin Additive (pentene-1/n-octane)

The reactivity of olefins in a fuel was determined by studying a binary fuel consisting of 95 mole % n-octane + 5 mole % pentene-1. The experimental data is summarized in Table 3. Colums 4 and 7 give the exhaust composition of the cell and the current contribution for pentene-1, respectively. A comparison of columns 1 and 4, the pentene-1 inlet and exhaust concentrations, respectively, shows that the olefin is preferentially oxidized irrespective of the fuel flow rate. As for the case with benzene, this indicates that the olefin is consumed as rapidly as it is supplied for the range of flow rates studied, and provided that $I_T > I_{ol}$.

The average values of the current contribution from penten-1, are plotted against the pentene-1 flow rate in Figure 4. It can be seen that there is a linear relationship between the current, I_{ol}, and flow rate, and since there is virtually no pentene-1 in the exhaust, the current produced is the stoichiometric amount calculcated from its flow rate. It is noted that at the higher flow rates there is a curvature towards the abscissa. This suggests that at high flow rates or high concentrations of the olefin the current from this compound will probably reach a limiting value.

The current contribution from pentene-1 for these reaction conditions and at low flows, as determined from Figure 4, can be expressed as:

$$I_{ol} = 4.83 \times 10^4 V_{ol} \quad (3)$$

Table 3

Current Contribution and Exhaust Composition for Pentene-1

Inlet Fuel Composition, mole %	Liquid Fuel Flow Rate, μl/min.	Pentene-1 Flow Rate, moles/min. x 10^6	Pentene-1 Concentration in Exhaust, mole % x 10^1	Total Current, I_T, amp	Anode Potential vs. H_2/H^+, volt	Current from Pentene-1 I_{o1}, amp	
95% n-octane + 5% Pentene-1	5	1.58	2.82	1.00	0.445	0.074	
	10	3.16	0.054	1.00	0.483	0.152	
	10	3.16	0.067	1.00	0.485	0.152	
	10	3.16	0.058	1.00	0.520	0.152	
	10	3.16	0.060	1.00	0.496	0.152	Ave.
	20	6.31	0.043	2.00	0.535	0.304	
	20	6.31	0.037	2.00	0.510	0.304	
	20	6.31	0.033	1.50	0.505	0.304	
	20	6.31	0.030	1.50	0.525	0.304	
	20	6.31	0.075	1.50	0.475	0.304	
	20	6.31	0.077	1.50	0.475	0.304	
	20	6.31	0.109	1.00	0.480	0.304	
	20	6.31	0.114	1.00	0.475	0.304	
	20	6.31	0.174	0.50	0.475	0.304	
	20	6.31	0.153	0.50	0.515	0.304	
	20	6.31	0.105	0.50	0.510	0.304	
	20	6.31	0.124	0.50	0.525	0.304	
	20	6.31	0.090	----	0.500	0.304	Ave.
	30	9.47	0.100	0.99	0.525	0.456	
	30	9.47	0.112	0.99	0.525	0.456	
	30	9.47	0.106	0.99	0.525	0.456	Ave.
	40	12.6	3.06	1.00	0.550	0.575	

where V_{o1} is the pentene-1 flow rate in gm mole/min. If the results are generalized to apply to all olefins the following result is obtained:

$$I_{o1} = nF \, u \, N_{o1} \tag{4}$$

where the symbols have the same meaning as described above for benzene.

3. Naphthene Additive (cyclohexane/n-octane)

Experiments to determine the relative reactivity of cyclohexane-type naphthenes and n-octane were conducted on a binary fuel consisting of 95 mole % n-octane and 5 mole % cyclohexane. The experimental results are summarized in Table 4.

The cyclohexane-type naphthenes are considerably different from the aromatic and the olefin compounds previously discussed. By comparing columns 1 and 4 which show the cyclohexane concentration in the inlet and exhaust streams, respectively, it is seen that only 27 to 44% of the naphthene is removed. This is in marked contrast to the aromatics and olefins which were virtually entirely removed (93 to 100%). However, it is of importance to note that the cyclohexane concentration in the exhaust is always substantially lower than the inlet concentration. This is shown in Figure 5 in which the cyclohexane concentration in the exhaust is plotted against the liquid fuel flow rate. It is seen that the cyclohexane concentration levels out at about 44% of the inlet concentration.

From a consideration of thermodynamic equilibrium data (4) for the gas phase dehydrogenation reaction:

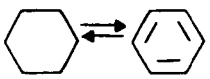

(5)

it shows that, for the conditions prevailing at the anode, the product of Reaction (5) will contain 2.3 mole % benzene and 2.7 mole % cyclohexane. The benzene (and hydrogen) will be rapidly and almost completely consumed.

From these equilibrium considerations, 46% of the naphthene would be consumed with some consumption of the accompanying cyclohexane. This compares favorably with the experimental values ranging from 56 to 72% (Table 4). The agreement with the low value (56%) obtained at the higher flow rates is in better agreement since under high flow conditions the electrochemical utilization of cyclohexane is lower than under low flow conditions.

Table 4

Current Contribution and Exhaust Composition for Cyclohexane

Inlet Fuel Composition Mole %	Liquid Fuel Flow Rate, μ l/min.	Cyclohexane Flow Rate, mole/min. x 10^6	Cyclohexane Concentration in Exhaust, mole %	Total Current, I_T, amp	Anode Potential vs. H_2/H^+, volt	Current from Cyclohexane, I_N, amp	
95% n-octane + 5% cyclohexane	10.7	3.34	1.39	0.800	0.475	0.148	
	10.7	3.34	1.37	0.800	0.485	0.149	
	10.7	3.34	1.35	0.800	0.485	0.149	
	10.7	3.34	1.37	0.800	----	0.149	Ave.
	20	6.25	1.94	0.990	0.525	0.236	
	20	6.25	1.98	0.990	0.525	0.233	
	20	6.25	1.99	0.980	0.525	0.233	
	20	6.25	1.97	0.987	----	0.234	Ave.
	30	9.37	1.89	0.980	0.510	0.352	
	30	9.37	2.01	0.960	0.540	0.339	
	30	9.37	1.93	0.960	0.510	0.347	
	30	9.37	1.94	0.967	-----	0.346	Ave.
	40	12.5	2.23	0.980	0.540	0.419	
	40	12.5	2.19	0.970	0.500	0.426	
	40	12.5	2.20	0.960	0.510	0.423	
	40	12.5	2.21	0.970	-----	0.423	Ave.

The average values of the current contribution from the naphthene I_N, is plotted vs. the naphthene flow rate in Figure 6. A linear relationship is again obtained as with benzene and pentene-1, but here it is noted that the line does not pass through the origin.

The experimental results in Figure 6 can be fitted to the following empirical equation:

$$I_N = 0.05 + 3.55 \times 10^4 V_N \quad (6)$$

where V_N is the flow rate of cyclohexane in mole/min.

Once again, if the results are generalized to all cyclohexane-type naphthenes the following relationship is obtained:

$$I_N = nF (8.65 \times 10^{-7} + 0.613 \mu N_N) \quad (7)$$

when N_N is the mole fraction of the naphthene at the inlet and the other terms have the significance described above.

B. Five Component Fuel

A fuel consisting of 74 mole % n-octane + 15 mole % methylcyclopentane + 5 mole % methylcyclohexane + 5 mole % pentene-1 + 1 mole % m-xylene was studied to determine whether the results reported above using binary fuels are applicable to more complex fuels. It is possible that one or more of the components are selectively oxidized at the expense of the others. A fuel of this particular composition was chosen since it was previously shown (1) to behave very similarly to pure n-octane. Furthermore, this study comes closer to simulating operations with a real commercial fuel. The experimental results are given in Table 5.

For the sake of better resolution in the chromatographic analysis, benzene and cyclohexane, which had been used as model additives in studies with binary fuels, were replaced by m-xylene and methylcyclohexane, respectively. The results should not be greatly affected. The exhaust compositions of the five fuel components are shown as a function of liquid fuel flow rate in Figures 7 thru 11. It is important to note that the n-octane concentration in the fuel actually increases from 74 to 96 mole % after a single pass through the cell as is shown in Figure 7. The naphthene concentrations for both the five and six-membered ring types are substantially reduced in the exhaust stream, especially at low fuel flow rates; this is shown in Figures 8 and 9.

Figures 10 and 11 show the pentene-1 and m-xylene concentrations in the exhaust, respectively, plotted as a function of liquid fuel flow rate.

Table 5

Current Contributions and Exhaust Composition of Components of a Synthetic Fuel

Inlet Fuel Composition, mole %: 74% n-octane + 15% methylcyclopentane + 5% methylcyclohexane + 5% pentene-1 + 1% m-xylene

Liquid Fuel Flow Rate, μl/min.	10	20	30	40
Octane Flow Rate, moles/min. x 10^6	49.16	98.32	147.5	196.6
MCP Flow Rate, moles/min. x 10^6	9.92	19.8	29.8	39.7
MCH Flow Rate, moles/min. x 10^6	3.32	6.64	9.96	13.28
Pentene-1 Flow Rate, mole/min. x 10^6	3.32	6.64	9.96	13.28
Xylene Flow Rate, mole/min. x 10^6	0.664	1.33	1.99	2.66
n-Octane Concentration, mole %	95.6	85.0	83.0	80.7
MCP Concentration, mole %	3.49	11.7	13.1	14.1
MCH Concentration, mole %	0.822	2.84	3.19	4.17
Pentene-1 Concentration, mole %	0.0581	0.267	0.534	0.774
M-Xylene Concentration, mole %	0.000	0.177	0.226	0.273
Total Current, amp	1.20	1.45	1.50	1.50
Anode Potential, volt	0.550	0.550	0.590	0.580
I_p, Octane-amp	0.320	0.422	0.268	0.267
I_N, MCP-amp	0.479	0.405	0.396	0.326
I_{N2}, MCH-amp	0.198	0.239	0.292	0.217
I_{ol} Pentene-1, amp	0.159	0.306	0.436	0.551
I_A, M-Xylene, amp	0.0449	0.0768	0.108	0.135

As for the case of binary fuels, the unsaturated compounds are virtually entirely depleted from the fuel stream at low fuel flow rates (approximately 10 µl/min.). The breakthrough of these compounds above these flow rates must be a result of competition for surface sites between the various fuel component molecules. However, the concentrations of these compounds are greatly reduced; thus, better than 70% removal of the aromatic compound and better than 80% of the olefin is observed. This fact is extremely significant, since it indicates that the more harmful components are preferentially oxidized resulting in an "exhaust fuel" that is richer in the more desirable components.

The current contributions of the five components under consideration are shown in Figures 12 thru 16. They were obtained by means of the simultaneous solution of five linear equations (2). Unfortunately, the solutions are quite sensitive to relatively small variations in each of the variables. Thus, an experimental error of about 1 to 3% in the chromatographic analysis can cause rather severe distortions in the calculated current contributions of the components for which the errors were made. Furthermore, the assumptions made for the parameter n (number of gm-equivalents/gm-mole) of each species and for the Faradiac efficiency, which was assumed to be 100%, will also influence the results.

These comments are pertinent, in view of the curve discontinuities observed in Figures 12 thru 14. These discontinuities were unexpected, considering the smooth variation of the exhaust composition data with flow rate (Figures 7 thru 9).

On the other hand, the relative reactivity of olefins and aromatics yield results as exhibited in Figures 15 and 16. These results are reminiscent of the binary fuel results and reflect the situation where it was shown that there is not necessarily an additive effect on performance when two or more "refractory" additives are present in a given fuel (1).

It is clear from the above discussion that the current contributions from n-octane, methylcyclopentane, and methylcyclohexane are difficult to calculate. This is not the case, however, for m-xylene and pentene-1. The current contributions for each of these components, at low flow rates, are given by the equations:

$$I_{ol} = 0.963\ nF\ \mu N_{ol} \qquad (8)$$

$$I_{A} = 0.93\ nF\ \mu N_{A} \qquad (9)$$

Equations (8) and (9) are in very good agreement with Equations (2) and (4) which apply to binary fuels. It should be noted that a different aromatic

additive was used in the binary mixture. This is an alternate way of expressing the fact that the electrochemical oxidation of olefins and aromatics at low fuel flow rates appears to proceed independent of the other species present in the fuel.

C. General Considerations

Figure 17 shows that aromatics, olefins, and naphthenes in pure form exhibit considerably poorer polarization characteristics than n-octane when oxidized electrochemically.

The rather unexpected relative reactivities observed in the present work for fuel mixtures is, therefore, probably due to competitive adsorption effects, with the more refractory species achieving high coverages of the active sites and being selectively oxidized. Unfortunately, no electrosorption data are available for the classes of compounds studied to put this discussion on a more quantitative basis.

Discussion

A clearer understanding of the preceding results can be obtained from some fundamental relationships. Consider an anode compartment of thickness t, containing an electrode of area A, as is shown in Figure 18. There is a steady flow, μ, of reactant mixture expressed as moles per unit time. A volume element, dA, is selected so that the concentration of component i is N_i expressed as mole fraction and the concentration leaving is $N_i - dN_i$. The rate of change in the number of moles of component i at a given point in the anode compartment, m_i, can be expressed by the equation:

$$\frac{dm_i}{dt} = \mu dN_i + r_i \, dA \qquad (10)$$

where r_i is the rate of oxidation of component i in the anode compartment expressed as moles of reactant converted per unit area of electrode per unit time, and the remaining symbols have their usual significance.

Considering the anode compartment as a flow reactor at steady-state, Equation (10) simplifies to:

$$r_i \, dA = -\mu dN_i \qquad (11)$$

Considering mainly activation effects and expressing the current density of a component i in terms of the reaction rate, we obtain:

$$i_i = n_i F r_i \qquad (12)$$

Combining Equations (11) and (12) and integrating yields:

$$\int_{o}^{A} dA = -nF\mu \int_{N_o}^{N} \frac{dN}{i} \tag{13}$$

here the subscript i has been eliminated for sake of simplicity and N_o is the mole fraction of the component under consideration at the inlet.

Expressing the current density in terms of the electrochemical kinetics of an activation-limited, anodic, forward reaction

$$\left| \eta_a \right| >> \frac{RT}{nF},$$

where η_a is the anodic activation polarization, we can write

$$i = nFN^{\gamma}k \exp\left(\frac{-\Delta G^*}{RT}\right) \exp\left(\frac{-\alpha nFE^o}{RT}\right) \exp\left(\frac{(1-\alpha)nF\eta_a}{RT}\right) \tag{14}$$

where γ is the reaction order, k is a rate constant, ΔG^* is the standard free energy of activation, E^o is the reversible potential, and α is the transfer coefficient. It is recognized that Equation (14) is the correct kinetic expression for the hydrocarbons studies, but for our purposes the following simplified equation can be

$$i = k' N^{\gamma} e^{\beta E} \tag{15}$$

more easily fitted to the experimental data, where k' and β are now constants to be fit to the experimental data. Substituting Equation (15) into Equation (13) yields:

$$\int_{o}^{A} dA = \frac{-nF\mu e^{-\beta E}}{k'} \int_{N_o}^{N} \frac{dN}{N^{\gamma}} \tag{16}$$

where upon integration and rearrangement gives:

$$\frac{k'A(1-\gamma)}{nF\mu} e^{\beta E} = N_o^{(1-\gamma)} - N^{(1-\gamma)} \tag{17}$$

for the case where $\gamma \neq 1$. Since none of the additives studied have a reaction order of unity this case was not considered. The constants in Equation (17) are listed in Table 6 for the additives studied.

Table 6

Constants for Equation (17)

Compound	k', ASF	β	γ
Benzene	0.039	9.3	-0.11
m-xylene	0.17	6.7	-0.11*
Methylcyclohexane	0.029	11.4	
Pentene-1	0.26	9.3	-0.16*
n-octane	0.12	13.1	~0.5

The empirical constants k' and β were determined from the linear portion of curves in Figure 19. The reaction order for benzene was given in a recent study by Bockris et. al. (5) and the values of the orders for m-xylene and pentene-1 were estimated from Bockris's data. The other values for γ were obtained by fitting the binary fuel data to Equation (17). Equation (17) permits the calculation of the exhaust composition of any compound for which the constants are known. It is hoped that the constants for various compounds in a particular class will be sufficiently similar to make Equation (17) general enough to calculate the exhaust composition (and therefore current contribution) of a fuel cell anode at any given set of anode operating conditions.

The fit of the experimental data for the five component fuel to Equation (17) is only fair if the condition:

$$e^{\beta E} \leq \frac{nF\mu N^{(1-\gamma)}}{k' A (1-\gamma)} \qquad (19)$$

is obeyed. The utilization of the components that were believed to be unreactive prior to this investigation can be explained by Equation (18), indicating that the results obtained can be explained from simple fundamental considerations.

Conclusions

1. Under anode operating conditions that present-day direct hydrocarbon fuel cell technology permits, the components of a practical fuel (aromatics, olefins, and to a certain extent naphthenes) can be preferentially oxidized. This is apparently a result of the magnitude of the relative coverage of the active sites with the components in question. The anode effluent becomes enriched in the more desirable paraffin component.

2. The preferential oxidation of the "unreactive" components can be explained by simple kinetic considerations.

The engineering significance of these findings is extremely important since it is now evident that no fuel pretreatment beyond established limits is necessary and that the fuel can be recycled without any harmful side effects.

Acknowledgements

This work is a part of the program under contract DA44-009-AMC-479(T) with the U.S. Army Engineer and Development Laboratories, Ft. Belvoir, Virginia, to develop a technology which facilitates the design and fabrication of practical military fuel cell power plants for operation on ambient air and hydrocarbon fuels.

The authors are grateful for the able assistance of Mr. Lucien Brassard who performed much of the experimental work.

References

1. Technical Summary Report No. 9, Hydrocarbon-Air Fuel Cells, January 1965-June 1966, ARPA Order No. 247, Contract Nos. DA44-009-ENG-4909, DA44-009-AMC-479(T), and DA44-009-ENG-4853, p. 2-107 et. seq.

2. Technical Summary Report No. 10, Hydrocarbon-Air Fuel Cells, July 1966-December 1966, ARPA Order No. 247, Contract Nos. DA44-009-ENG-4909, DA44-009-AMC-479(T), and DA44-009-ENG-4853, p. 4-27 ff.

3. L. W. Niedrach and H.R. Alford, J. Electrochem. Soc., 112, 117 (1965).

4. F.D. Rossini et. al., "Selected Values of Properties of Hydrocarbon", Circular C461 N.B.S. 1947.

5. J.O.M. Bockris, et. al., Trans. Faraday Soc., 61, 515, 1965.

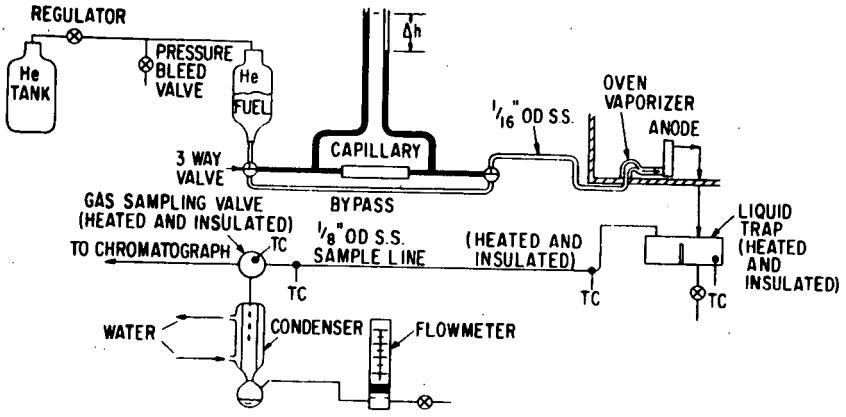

Figure I Fuel Feed and Exhaust for Chromatographic Study of Binary Fuels.

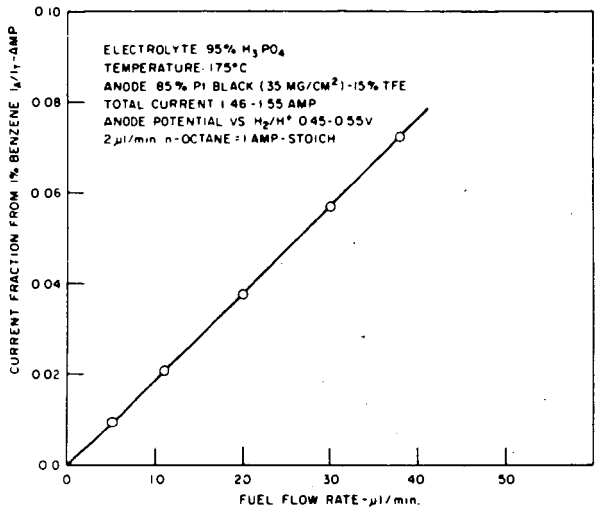

Figure 2. Current Fraction from Benzene vs. Fuel Flow Rate

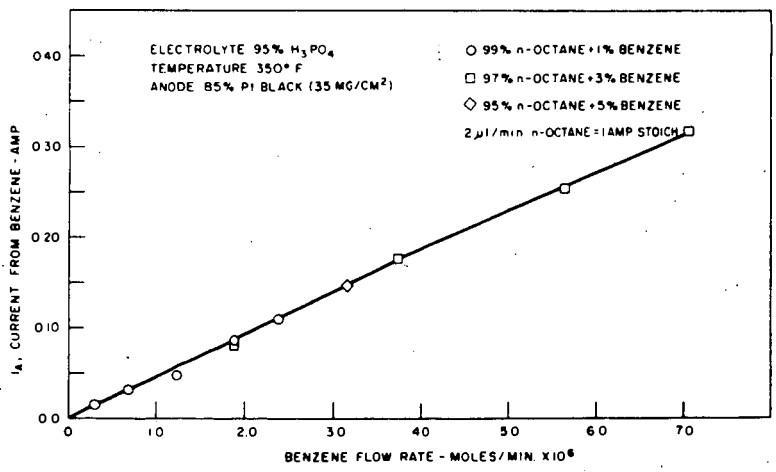

Figure 3 Current from Benzene vs. Benzene Flow Rate for Fuels Containing 1-5 mole % Benzene

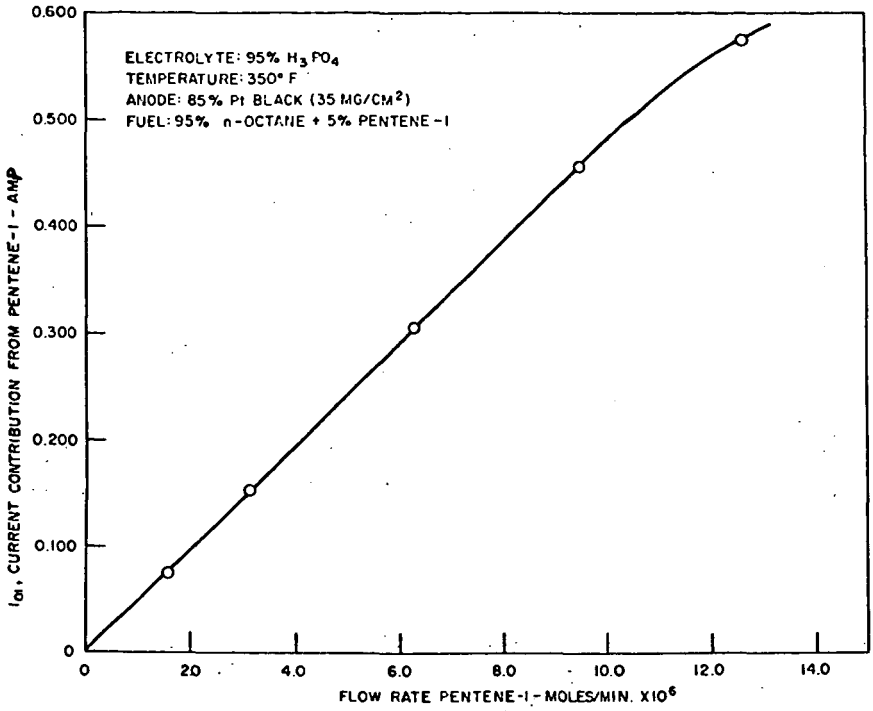

Figure 4 Current Contribution from Pentene-1 vs. Pentene-1 Flow Rate from a Fuel Containing 5 mole % Pentene-1

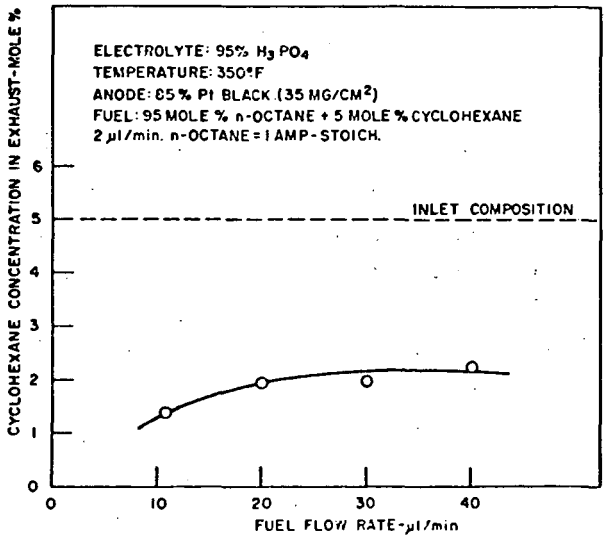

Figure 5 Effect of Liquid Fuel Flow Rate on Cyclohexane Concentration in Exhaust for a Fuel Containing 5 mole % Cyclohexane at Inlet

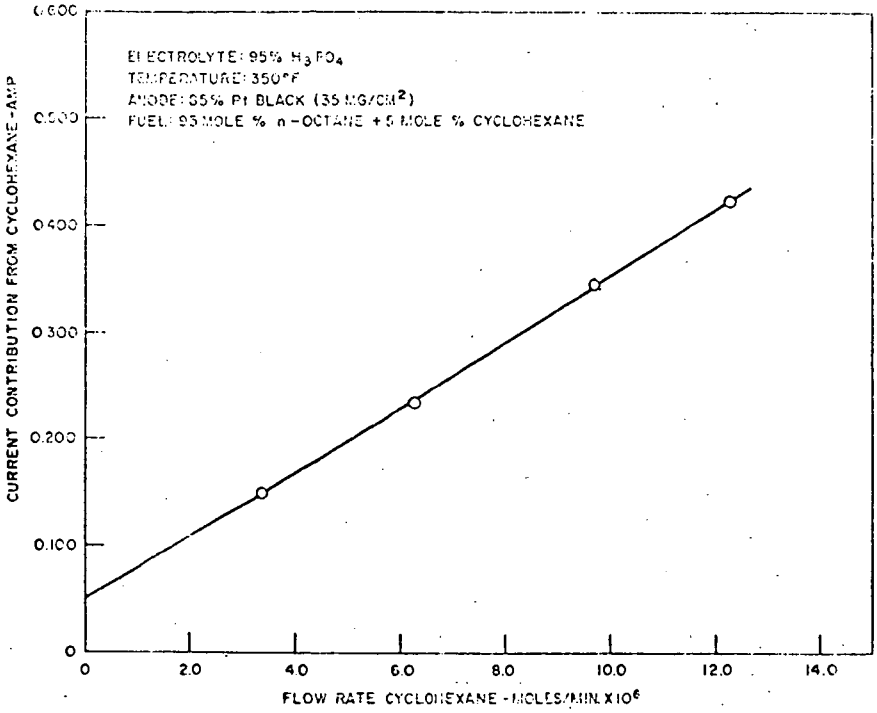

Figure 6 Current Contribution from Cyclohexane vs. Cyclohexane Flow Rate for a Fuel Containing 5 mole % Cyclohexane

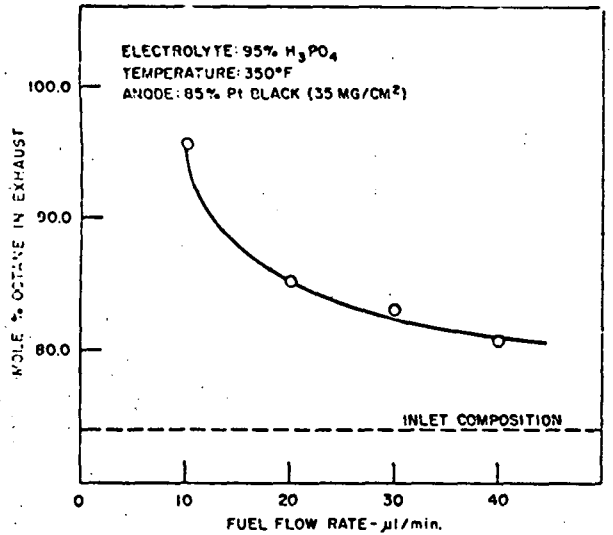

Figure 7 Effect of Liquid Fuel Flow Rate on Octane Concentration in Exhaust for a Fuel Containing 74% n-Octane + 15% Methylcyclopentane + 5% Methylcyclohexane + 5% Pentene-1 + 1% M-Xylene

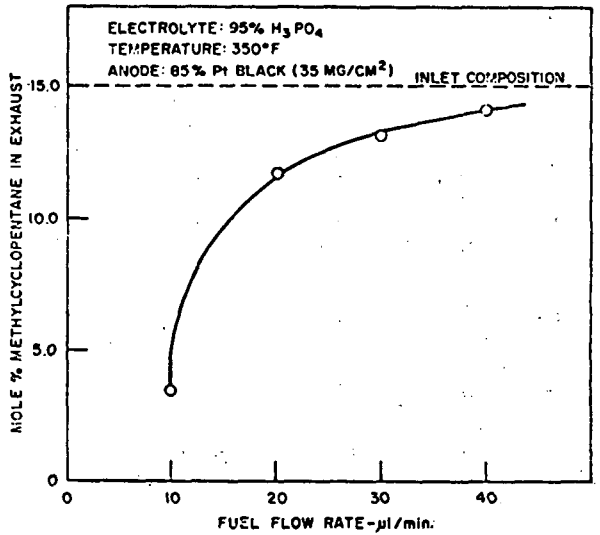

Figure 8 Effect of Liquid Fuel Flow Rate on Methylcyclopentane Concentration in Exhaust for a Fuel Containing 74% n-Octane + 15% Methylcyclopentane + 5% Methylcyclohexane + 5% Pentene-1 + 1% M-Xylene

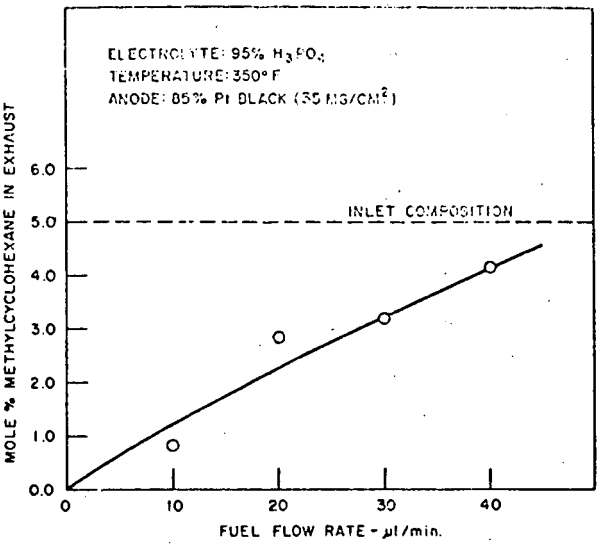

Figure 9 Effect of Liquid Fuel Flow Rate on Methylcyclohexane Concentration in Exhaust for a Fuel Containing 74% n-Octane + 15% Methylcyclopentane + 5% Methylcyclohexane + 5% Pentene-1 + 1% M-Xylene

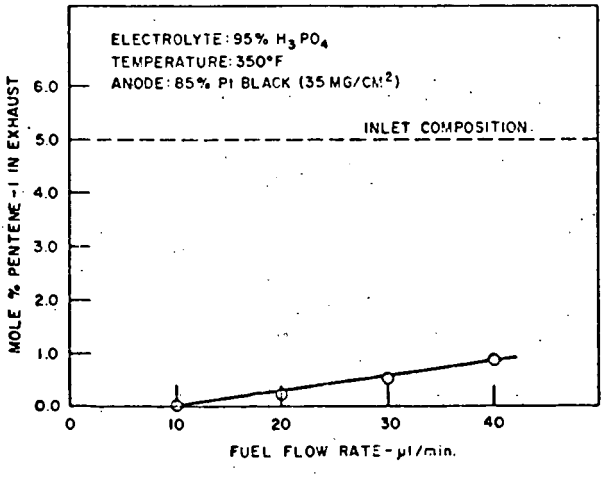

Figure 10 Effect of Liquid Fuel Flow Rate on Pentene-1 Concentration in Exhaust for a Fuel Containing 74% n-Octane + 15% Methylcyclopentane + 5% Methylcyclohexane + 5% Pentene-1 + 1% M-Xylene

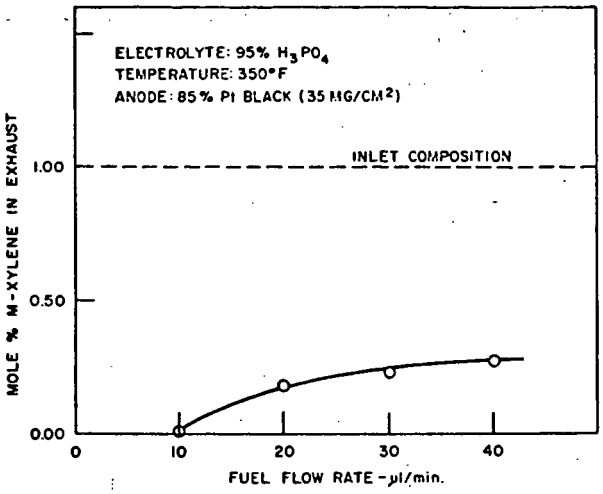

Figure 11 Effect of Liquid Fuel Flow Rate on M-Xylene Concentration in Exhaust for a Fuel Containing 74% n-Octane + 15% Methylcyclopentane + 5% Methylcyclohexane + 5% Pentene-1 + 1% M-Xylene

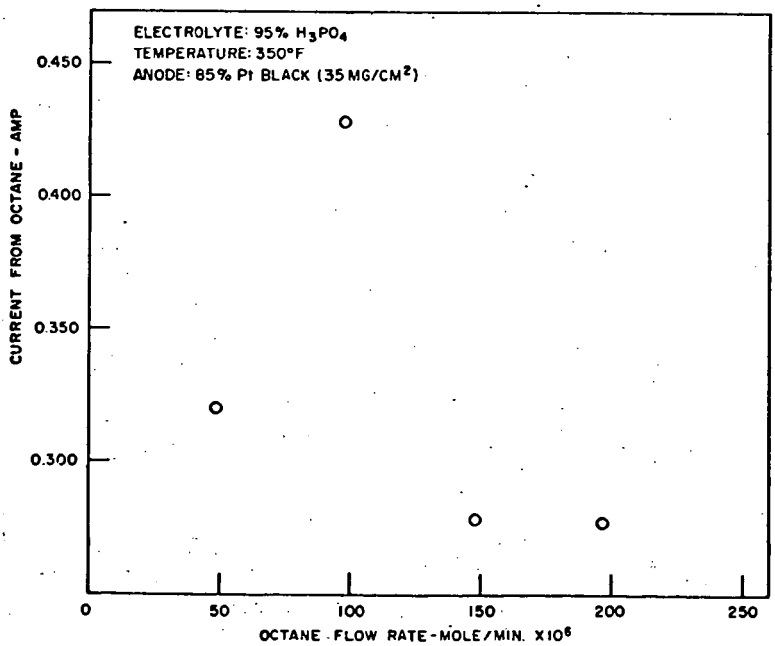

Figure 12 Effect of Octane Flow Rate on Current Contribution from Octane for Fuel Containing 74% n-Octane + 15% Methylcyclopentane + 5% Methylcyclohexane + 5% Pentene-1 + 1% M-Xylene

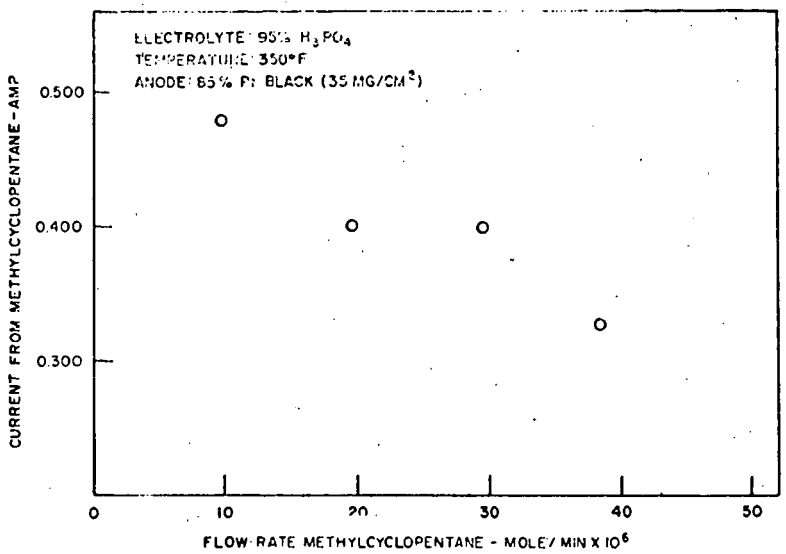

Figure 13 Effect of Methylcyclopentane Flow Rate on Current Contribution from Methylcyclopentane for Fuel Containing 74% n-Octane + 15% Methylcyclopentane + 5% Methylcyclohexane + 5% Pentene-1 + 1% N-Xylene

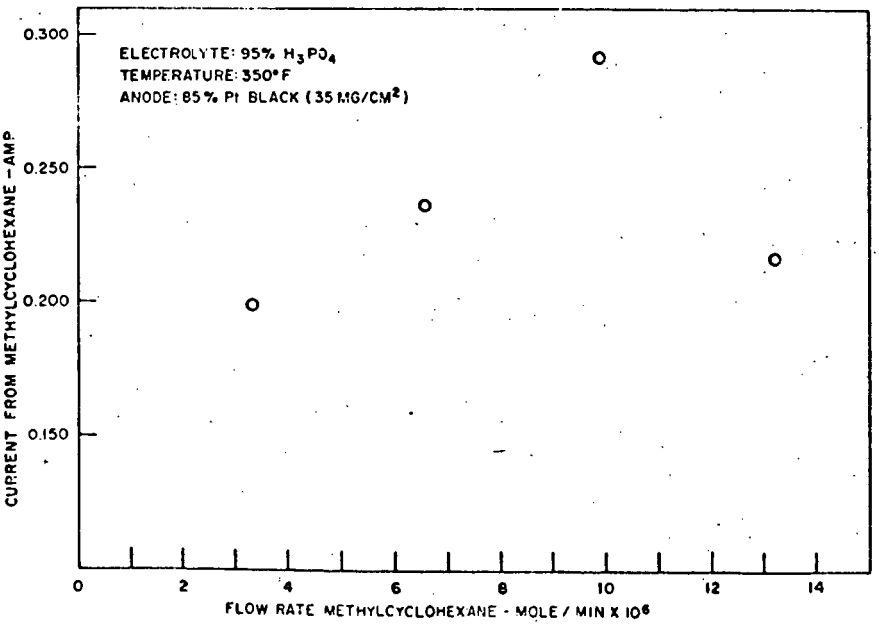

Figure 14 Effect of Methylcyclohexane Flow Rate on Current Contribution from Methylcyclohexane for Fuel Containing 74% n-Octane + 15% Methylcyclopentane + 5% Methylcyclohexane + 5% Pentene-1 + 1% M-Xylene

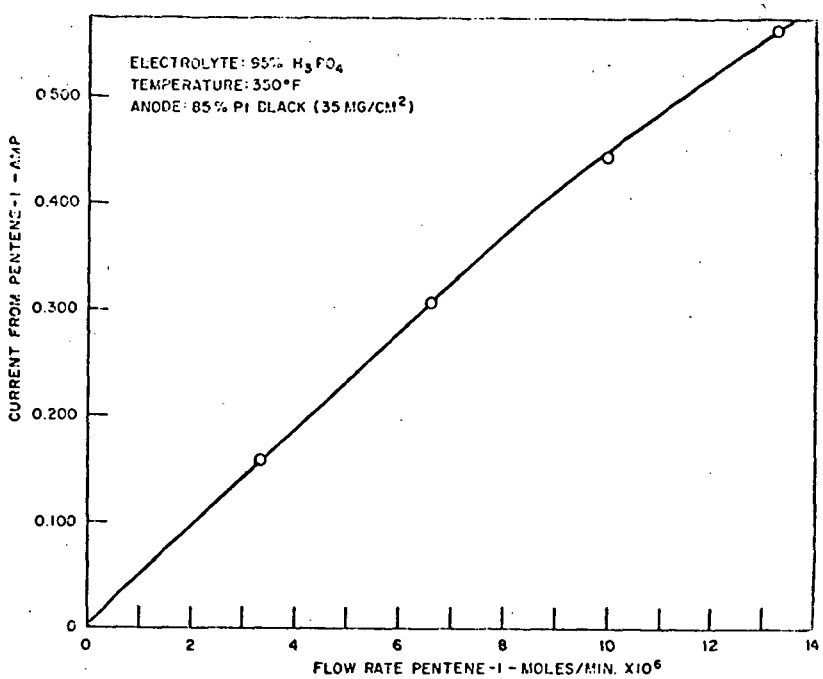

Figure 15 Effect of Pentene-1 Flow Rate on Current Contribution from Pentene-1 for Fuel Containing 74% n-Octane + 15% Methylcyclopentane + 5% Methylcyclohexane + 5% Pentene-1 + 1% M-Xylene

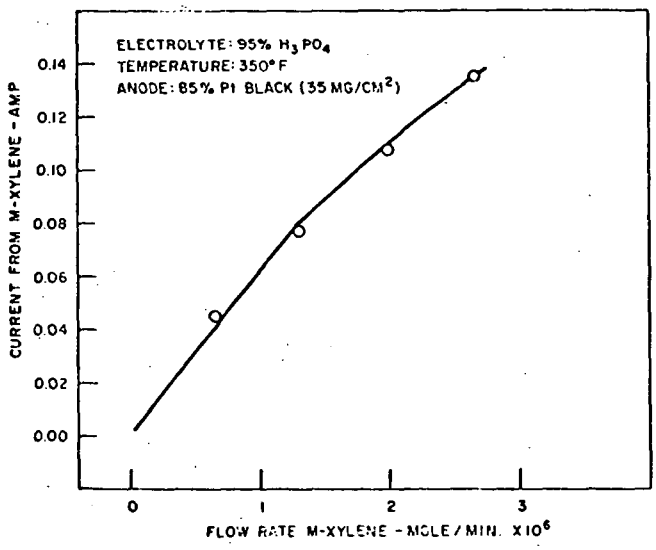

Figure 16 Effect of M-Xylene Flow Rate on Current Contribution from M-Xylene for Fuel Containing 74% n-Octane + 15% Methylcyclopentane + 5% Methylcyclohexane + 5% Pentene-1 + 1% M-Xylene

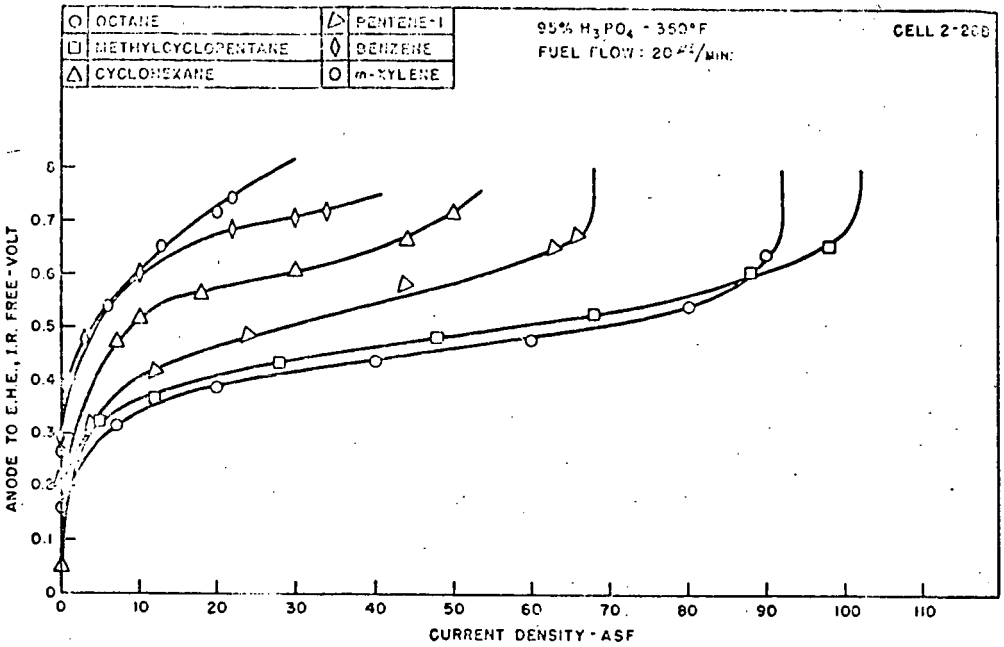

Figure 17 Polarization Curves for n-Octane, Methylcyclopentane, Cyclohexane, Pentene-1, Benzene, and M-Xylene

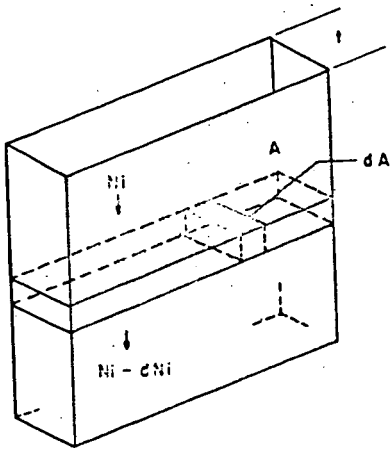

Figure 18 Fuel Cell Anode Compartment

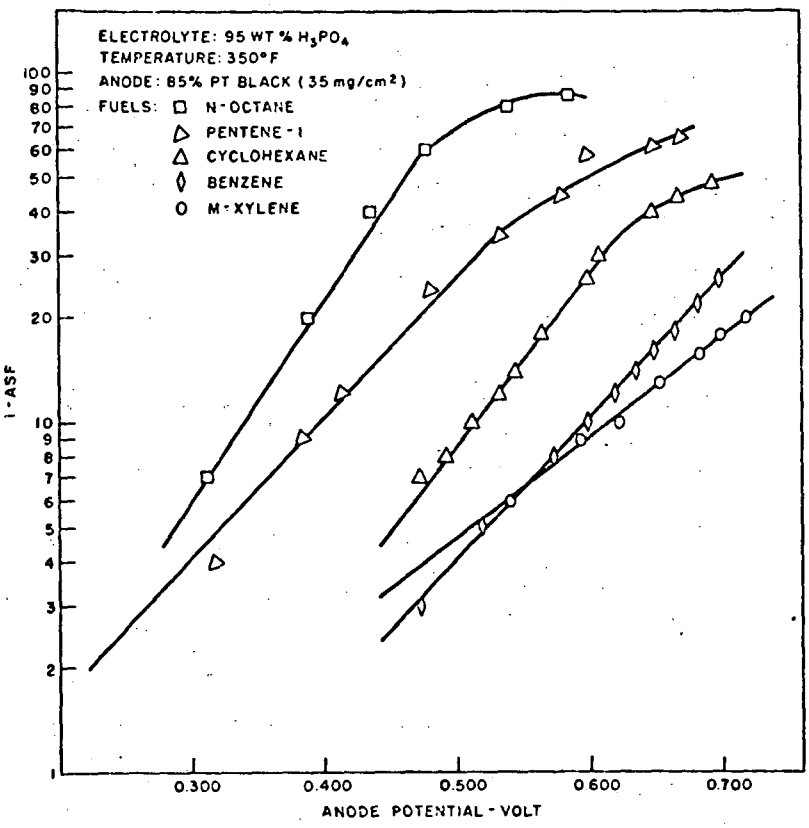

Figure 19 Current Density vs. Anode Potential for n-Octane, Pentene-1, Cyclohexane, Benzene, and M-Xylene